Am J Cancer Res 2023;13(2):394-407
www.ajcr.us /ISSN:2156-6976/ajcr0146811

Original Article

Moxibustion attenuates liver metastasis of colorectal cancer by regulating gut microbial dysbiosis

Ya-Fang Song[1,3*], Jin-Yong Zhou[2*], Yi Zhuang[1], Jing Guo[1], Xu-Dong Wang[1], Yu-Hang Wang[1], Ting-Ting Zhao[3], Lu Chen[3], Hao Chen[1], Jian-Hua Sun[3], Li-Xia Pei[3]

[1]Department of Acupuncture and Massage, Health Preservation and Rehabilitation, Nanjing University of Chinese Medicine, Nanjing, Jiangsu, P. R. China; [2]Department of Central Laboratory, Affiliated Hospital of Nanjing University of Chinese Medicine, Nanjing, Jiangsu, P. R. China; [3]Department of Acupuncture Rehabilitation, Affiliated Hospital of Nanjing University of Chinese Medicine, Nanjing, Jiangsu, P. R. China. [*]Equal contributors.

Received October 1, 2022; Accepted January 12, 2023; Epub February 15, 2023; Published February 28, 2023

Abstract: The liver metastasis is the primary factor attributing to the poor prognosis of colorectal cancer (CRC). Moxibustion has been used clinically against multiple malignancies. In this study, we explored the safety, efficacy, and the potential functional mechanisms of moxibustion in modulating the liver metastasis of CRC by using GFP-HCT116 cells-derived CRC liver metastasis model in Balb/c nude mice. The tumor bearing mice were randomly divided into model control and treatment groups. Moxibustion was applied to the BL18 and ST36 acupoints. CRC liver metastasis was measured by fluorescence imaging. Furthermore, feces from all mice were collected, and 16S rRNA analysis was used to assess their microbial diversity, which was analyzed for its correlation with liver metastasis. Our results indicated that the liver metastasis rate was decreased significantly by moxibustion treatment. Moxibustion treatment also caused statistically significant changes in the gut microbe population, suggesting that moxibustion reshaped the imbalanced gut microbiota in the CRC liver metastasis mice. Therefore, our findings provide new insights into the host-microbe crosstalk during CRC liver metastasis and suggest moxibustion could inhibit CRC liver metastasis by remolding the structure of destructed gut microbiota community. Moxibustion may serve as a complementary and alternative therapy for the treatment of patients with CRC liver metastasis.

Keywords: Moxibustion, colorectal cancer, metastasis, gut microbiota, intrasplenic injection

Introduction

Colorectal cancer (CRC) is one of the most common malignant tumors and the second highest cause of cancer-related deaths worldwide [1, 2]. In China, the incidence and mortality of CRC rank fifth among all malignant tumors, and most of the patients were diagnosed at the middle-advanced stage. Although approximately 15-20% of patients with CRC have distant metastases at diagnosis [3], and 40 to 50% of patients with CRC eventually die of the liver metastasis [4], the treatment of CRC liver metastasis is still limited.

The gut microbiota has a complex relationship with immune response, tissue homeostasis, and diseases. The resident microbiota imbalance promotes chronic inflammation, immune subversion, and the production of carcinogenic metabolites. For example, Bacteroides fragilis toxin, colibactin, and cytotoxic necrotizing factors can induce several neoplastic changes known as the hallmarks of cancer. Recent studies have highlighted the key role of the gut microbiota in mediating the initiation and progression of CRC, via increasing the population of pathogenic bacteria at the expense of protective bacteria [5, 6].

Moxibustion, a form of heat therapy which is an important part of integrative medicine, has been recognized as a powerful tool in enhancing or coordinating the anti-tumor immune response in the last decade [7]. Moxibustion can help repair the abnormal intestinal microecology with a balanced bacterial species, composition, quantity, and biological activity, resulting in the restoration of healthy immune function in the body [8, 9]. Moxibustion exerts its

therapeutic effects through regulating the composition of microbiome in intestinal mucus, which increases the abundance of Firmicutes while reducing the abundance of Bacteroidetes as well as Proteobacteria [10]. However, little is known about how moxibustion regulates the composition of the intestinal microbes, thereby affecting CRC liver metastasis. Therefore, in this study, we hypothesized that moxibustion might be beneficial in suppressing the microbial populations of procarcinogenic microbiota. To test this, we used a splenic transplanta-tion of colon cancer cells model to examine the impact of moxibustion on liver metastasis. We also explored the potential mechanism involved in moxibustion's effect on liver metastasis from the aspect of the gut microbiota. Our findings provide a scientific basis for the therapeutic application of moxibustion in the treatment of CRC liver metastasis.

Materials and methods

Animals and establishment of liver metastasis model

Pathogen free male BALB/C nude mice (20-24 g, aged 4-6 weeks) were purchased from the Comparative Medicine Centre of Yangzhou University (Yangzhou, Jiangsu, China). The experimental protocol was approved by the Animal Ethics Committee of the Affiliated Hospital of Nanjing University of Chinese Medicine, and all experiments were performed strictly in accordance with the guidelines of the experimental protocol (Number: 2018 DW-03-03). CRC Liver metastasis mouse model was established using previously published protocols [11, 12]. Briefly, green fluorescent protein- expressing human colon cancer cells GFP-HCT-116 were cultured in Roswell Park Memorial Institute (RPMI)-1640 medium (containing 10% FBS) and maintained in a 37°C humidified incubator with 5% CO_2. To generate GFP-HCT-116 cells-derived CRC Liver metastasis mouse model, mice were first anesthetized with 25% chloramine ketone (1 μL/g, i.p.), and a 1-cm laparotomy was performed on the left subcostal region of the abdomen. The spleen was then gently exposed, and the GFP-HCT-116 cells (2×10^6 cells/mouse in 20 μL PBS) were implanted via intrasplenic injection into sixty nude mice. Afterward, the spleen was put back into the abdominal cavity, and the abdominal wall was sutured with 5.0 stitches. The mice were recovered on a heating pad after surgery and then returned to their housing cages. The overall condition, food intake, and weight change of these mice were monitored daily. At the end of the experiment, the liver and spleen were resected to investigate the primary tumor formation and liver metastasis. Tumor images were acquired under a fluorescence stereo microscope.

Group division and moxibustion implementation

Balb/c nude mice (n = 60) were randomly divided into four groups (n = 15/group): G1: control group (MC), G2: Pre-Mox group, G3: Post-Mox group, and G4: Pre-Post-Mox group. The treatment strategy for each group was as follows: G1: MC group: the model control group, no moxibustion treatment was administered. G2: Pre-Mox group: the moxibustion pretreatment group, mice received moxibustion treatment for 2 weeks before GFP-HCT-116 cell implantation. G3: Post-Mox group: the moxibustion posttreatment group, mice received moxibustion treatment for 3 weeks after GFP-HCT-116 cell implantation. G4: Pre-Post-Mox group: the moxibustion pretreatment + posttreatment group, mice received moxibustion treatment for 2 weeks before GFP-HCT-116 cell implantation plus 3 weeks after GFP-HCT-116 cell implantation for a total of 5-week moxibustion treatment.

Mice were fixed on the fixation device via tail fixation when moxibustion treatment was administered. The G1 MC group mice also received the same fixation but without any moxibustion treatment. For mild moxibustion treatment, bilateral Ganshu (BL18) and bilateral Zusanli (ST36) acupuncture points were selected based on the locations described in Experimental Acupuncture [13]. A moxa stick of 4 mm in diameter was ignited and placed 1.5 cm above the selected points for 10 min per day. The skin temperature of mice was about 42-44°C as measured by infrared thermometer. The experimental workflow is shown in **Figure 1**.

Tumor imaging

At the end of the study, all mice were sacrificed, and open fluorescent imaging was performed to carefully examine the formation of primary tumors and all liver metastases. A fluorescence stereo microscope (model MZ650, Nanjing

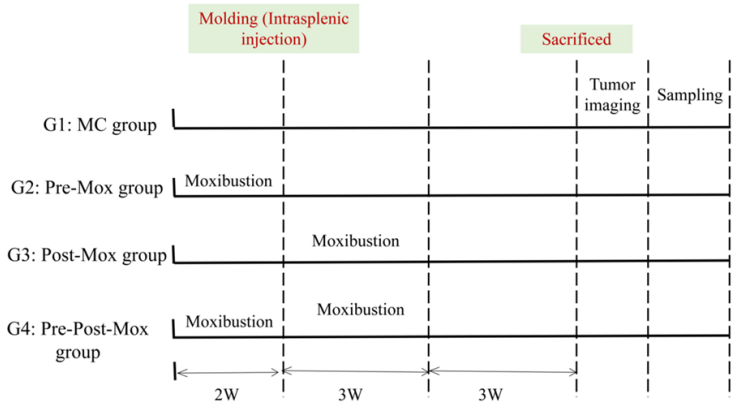

Figure 1. The flowchart of the experiment: Intervention timeline for four groups: G1: the model control group (MC, No moxibustion treatment), G2: the moxibustion pretreatment group (Pre-Mox, 2-week moxibustion treatment before the intrasplenic injection of GFP-HCT116 cells), G3: the moxibustion posttreatment group (Post-Mox, 3-week moxibustion treatment after GFP-HCT116 cell intrasplenic injection), G4: the moxibustion pretreatment + posttreatment group (Pre-Post-Mox, 2-week treatment before plus 3-week treatment after GFP-HCT116 cell intrasplenic injection). All mice were injected with 20 μL of 2 × 10^6 GFP-HCT116 cell suspension in the spleen. W: Week.

Optic Instrument Inc., Nanjing, China) equipped with a D510 long-pass emission filter (Chroma Technology, Brattleboro, VT, USA) and a cooled color charge-coupled device camera (Qimaging, BC, Canada) was used to acquire the images. Selective excitation of GFP was achieved using an illuminator equipped with a HQ470/40 band-pass filter. Images were processed and analyzed using Image Pro plus 6.0 software (Media Cybernetics, Silver Spring, MD, USA).

16S rRNA gene sequencing

The stool samples of mice were initially stored at 80°C freezer. DNA extraction, bacterial 16S rRNA gene amplification, and 454 pyrosequencing of 16S rRNA gene libraries were performed. The V4 hypervariable region of the 16S rRNA gene was amplified using primers 515F and 806R [14]. TruSeq® DNA PCR-Free Sample Preparation Kit (Illumina, San Diego, CA, USA) was used to construct the sequencing library. The constructed library was quantified by Qubit fluorometry (Thermo Fisher Scientific, Waltham, MA, USA) and PCR, and then sequenced using an Illumina NovaSeq-6000 instrument (Illumina, USA). Operational taxonomic units (OTUs) were clustered at 97% similarity, and chimeric sequences were removed using Uchime (https://drive5.com/https://drive5.com/).

Statistical analyses

Statistical analysis was performed using SPSS 24.0 software (IBM Corp., Armonk, NY, USA). Data were presented as means ± standard error of the mean (SEM). Fisher's precision probability test was used when comparing liver metastasis rates. One-way analysis of variance (ANOVA) and Student-Newman-Keuls (SNK) test were used for normally distributed data, while the least significant difference (LSD) test was performed to evaluate the parametric data. Wilcoxon test and Kruskal-Wallis H test with pairwise comparisons between groups were performed by rank-based ANOVA analysis for non-parametric data. Alpha diversity was determined by the Good's coverage, Chao1 index and Observed species, and Shannon diversity index. Beta diversity between different treatments was examined by performing a Principal Coordinate Analysis (PCoA) on Bray-Curtis dissimilarity distances. Visualization of the multidimensional distance matrix was achieved through either Multi-Dimensional Scaling (MDS) or its Non-Metric Multi-Dimensional Scaling (NMDS). Changes in the fecal microbiota composition were evaluated using a two-tailed t-test at different taxon levels. $P < 0.05$ was considered statistically significant.

Results

Moxibustion attenuated CRC liver metastasis in the nude mice

After splenic inoculation of GFP-HCT-116 cells in nude mice, the CRC liver metastasis was examined by a fluorescence optical imaging system. As shown in **Figure 2**, the green fluorescence clusters indicated tumor growth. If the metastasis did not occur, no green fluorescence signal would be detected in liver tissues. We detected a strong GFP signal in the livers of G1 MC group mice, indicating the strong liver metastasis. However, the metastasis rate decreased significantly from 100% (10/10 in MC group) to 50% (6/12) in G2 Pre-Mox group ($P = 0.009$), to 46% (6/13) in G3 Post-Mox

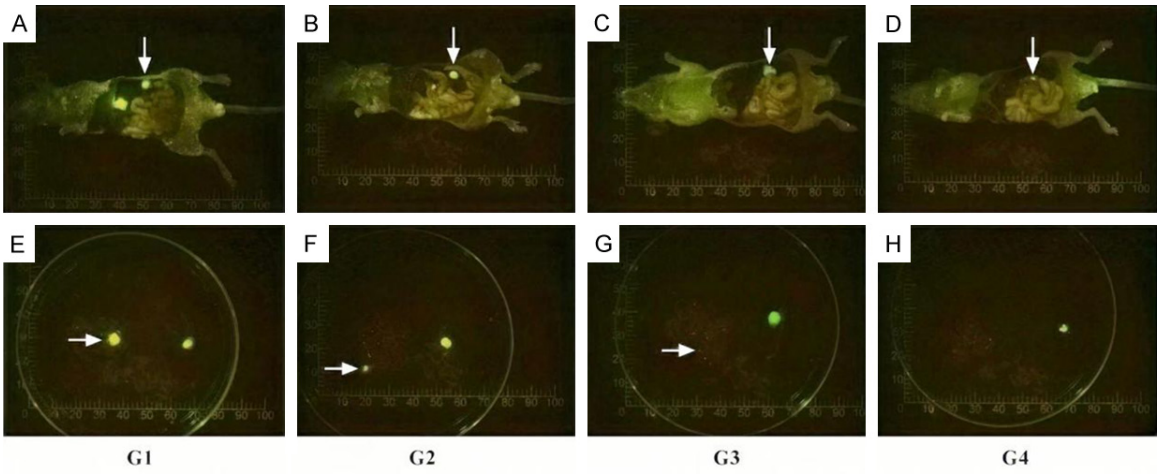

Figure 2. Representative images of CRC liver metastasis in the G1, G2, G3 and G4 groups. A-D. Images of mice anatomy showing the inner organs. The white arrows pointing down indicate the transplanted tumor in the spleen. E-H. The arrows pointing right indicate the metastatic tumors. A, E. G1: Model control (MC) group; B, F. G2: Pre-Mox group; C, G. G3: Post-Mox group; D, H. G4: Pre-Post-Mox group.

group (P = 0.005), and further to 25% (3/12) in G4 Pre-Post-Mox group (P = 0.000) (**Figure 3A**). Compared with the MC group, the number of liver metastatic tumor, primary spleen tumor volume, and spleen tumor weight in the Pre-Mox, Post-Mox, and Pre-Post-Mox groups were significantly decreased (P < 0.01), although the differences among the Pre-Mox, Post-Mox, and Pre-Post-Mox groups were not statistically significant (P > 0.05) (**Figure 3B-D**). As for the weight of the liver metastatic tumors, a similar trend was observed between the MC group and the Pre-Post-Mox group (P < 0.001, **Figure 3E**). These results suggest that moxibustion can inhibit the liver metastasis of CRC and that the mice in Pre-Post-Mox group have the lowest liver metastasis rate.

Moxibustion altered the richness and diversity of gut bacterial communities

Based on the sequencing analysis of fecal samples, a total of 3.9 million MiSeq paired reads were obtained from 46 samples, of which 3.78 million were classified into 1,956 OTUs. The analysis of α-diversity was performed to estimate fecal microbiome composition and diversity. The Good's coverage score revealed that the low abundant OTU coverage in the Pre-Mox, Post-Mox and Pre-Post-Mox groups did not increase significantly by moxibustion treatment compared with the MC group (P > 0.05, **Figure 4A**). Next, we used Chao1 and Observe species index to investigate the microbe species composition in the samples. As shown in **Figure 4B**, the Observed species index decreased significantly in the Pre-Post-Mox group mice compared with that of the MC mice (P = 0.0039). Furthermore, the observed species index in the Post-Mox and Pre-Post-Mox group mice was significantly decreased compared with that in the Pre-Mox group mice (P = 0.0078, P = 0.0014, respectively). Similarly, the Chao1 index was significantly lower in the Pre-Post-Mox mice than in the MC mice (P = 0.0203). Compared with the Pre-Mox group, the Post-Mox group had significantly decreased Chao1 index (P = 0.004), and a similar trend was observed in the Pre-Post-Mox group (P = 6e-04, **Figure 4C**). Together, these results suggest that moxibustion reduces the species richness. Nevertheless, Shannon's diversity index in the moxibustion-treated mice was not significantly affected compared with that in the MC mice (P > 0.05, **Figure 4D**).

Altered microbiome composition by moxibustion treatment

Beta diversity analysis was performed to estimate the microbial community composition among the mice in the 4 groups. Principal coordinates analysis (PCoA) and Bray-Curtis similarity cluster analysis, together with heatmap clustering based on OTU abundance were performed to provide an overview of the gut microbiota composition. As shown in **Figure 5A**, the beta diversity increased significantly in the Pre-Mox, Post-Mox, and Pre-Post-Mox group mice compared with that in the MC mice. A decreas-

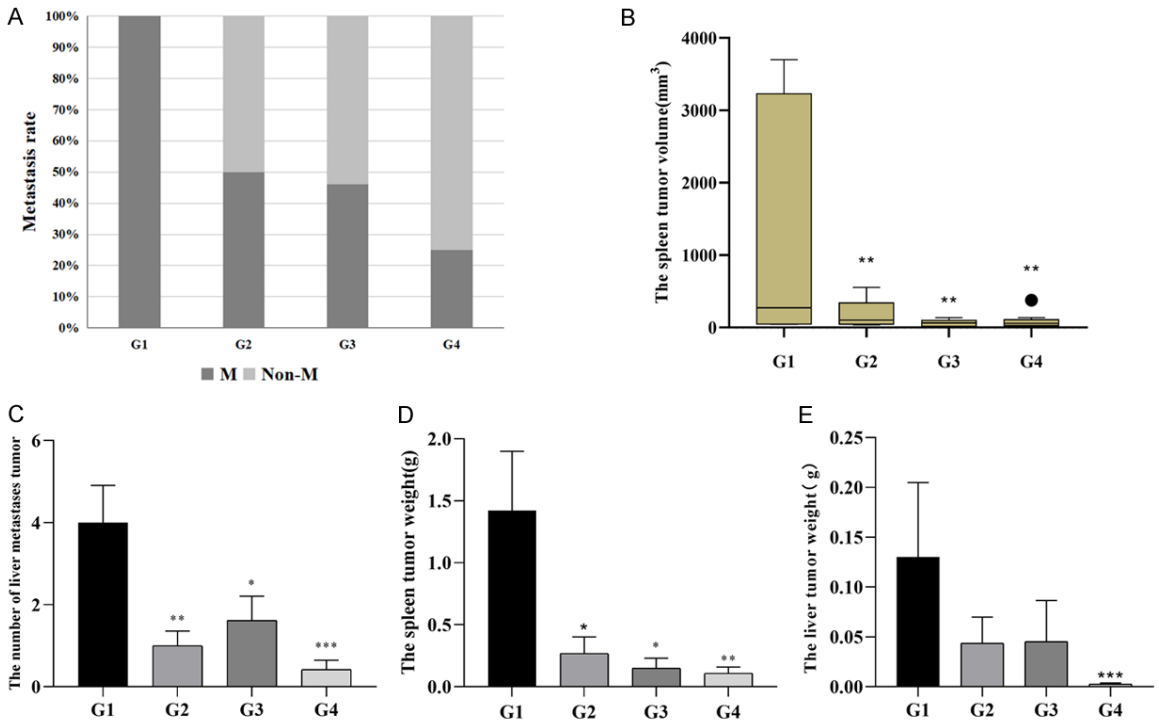

Figure 3. Examination of liver metastasis, spleen tumor volume, the number of metastatic tumors, the spleen tumor weight, and the liver metastatic tumor weight in different groups. A. Liver metastasis rates in different groups. M: metastasis. non-M: non-metastasis; G1: Model control (MC) group; G2: Pre-Mox group; G3: Post-Mox group; G4: Pre-Post-Mox group. B. Spleen tumor volume in all groups. C. The number of metastatic tumors in all groups. D. Spleen tumor weights in all groups. E. Liver metastatic tumors weights in all groups. The results were expressed as the mean ± SEM. $^{*}P < 0.05$; $^{**}P < 0.01$, $^{***}P < 0.001$ compared with the MC group.

ed trend was observed among the Pre-Mox, Post-Mox, and Pre-Post-Mox groups, with the beta diversity being obviously lower in the Post-Mox and Pre-Post-Mox groups than in the Pre-Mox group. PCoA showed that the first and second principal coordinates accounted for 42.78% and 11.91% of the total variations, respectively (**Figure 5B**). Non-Metric Multi-Dimensional Scaling (NMDS) demonstrated significant differences between the MC group and the Pre-Mox, Post-Mox, or Pre-Post-Mox groups with the stress as 0.11G (**Figure 5C**). The heat map in **Figure 5D** shows the difference between the clustering and prevalence of the 10 most abundant species at the phylum level. Taken together, these results confirm that the moxibustion altered microbial composition in the CRC liver metastasis nude mice.

Moxibustion treatment caused the alteration of microbiota at the levels of phylum, class, order, family, genus, and species

To further investigate what microbes contribute to the apparent differences in the diversity of gut microbiota and whether changes in gut microbiota are essential to the moxibustion-suppressed CRC liver metastasis, we thoroughly analyzed the alteration in microorganis-ms among the MC, Pre-Mox, Post-Mox, and Pre-Post-Mox groups at the levels of phylum, class, order, family, genus and species.

At the phylum level, the average abundance of Firmicutes was 64.4% in the MC group and 48.7% in the Pre-Post-Mox group ($P = 0.0253$). At the class level, Erysipelotrichia and Coriobacteriia in the Post-Mox group, while Verrucomicrobiae, Erysipelotrichia, Deltaproteobacteria, and unidentified Bacteria in the Pre-Post-Mox group were significantly more abundant compared to those in the MC mice ($P < 0.05$). Deltaproteobacteria were significantly less abundant in Pre-Mox and Post-Mox mice than in Pre-Post-Mox mice ($P < 0.05$, **Figure 6A**). At the order level, compared with the MC group, the abundances of Erysipelotrichales, Coriobacteriales, and unidentified Gammaproteobacteria were significantly higher, while Campylobacterales and Bifidobacteriales were significantly lower in the Post-Mox mice. In the Pre-Post-Mox

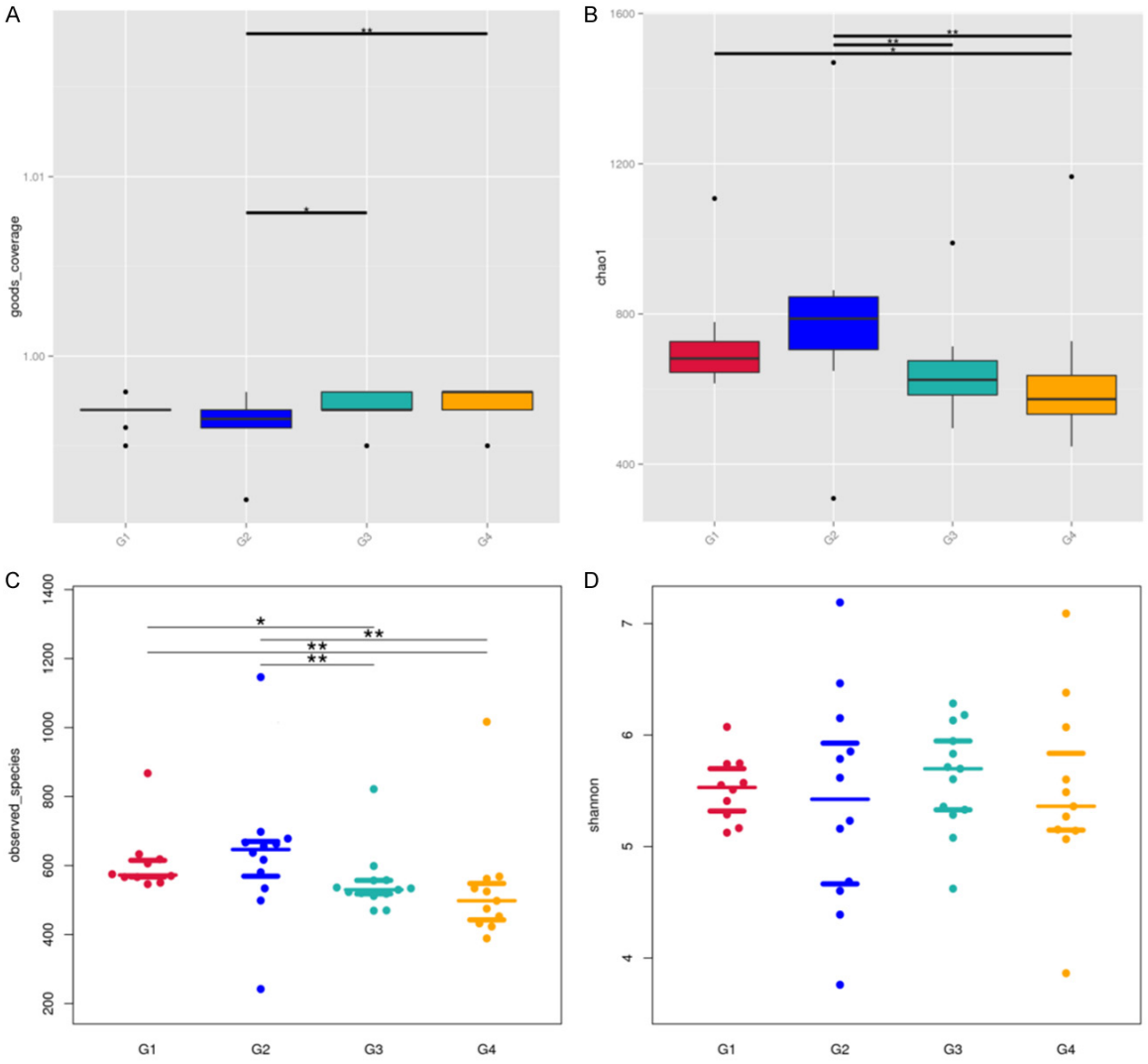

Figure 4. Comparison of α-diversity among G1, G2, G3 and G4 groups by using Good's coverage, Chao1 index, Observed species, and Shannon diversity index. A. Good's coverage; B. Chao1 index; C. Observed species; D. Shannon diversity index. $^{*}P < 0.05$; $^{**}P < 0.01$. Overall effects were identified by a Kruskal-Wallis test, and the different effects among treatments were determined by pairwise Wilcoxon rank sum tests. G1: MC group; G2: Pre-Mox group; G3: Post-Mox group; G4: Pre-Post-Mox group.

group, Verrucomicrobiales, Erysipelotrichales, Desulfovibrionales, unidentified Gammaproteobacteria were significantly more abundant, while Campylobacterales was less abundant compared with those in the MC group ($P < 0.05$, **Figure 6B**). Similarly, at the family level, Enterococcaceae was significantly enriched in the Pre-Mox mice; Muribaculaceae, Erysipelotrichaceae, Eggerthellaceae, Enterococcaceae, Burkholderiaceae, and Helicobacteraceae was enriched while Bifidobacteriaceae was less abundant in the Post-Mox mice. For the Pre-Post-Mox mice, compared to MC mice, Akkermansiaceae, Erysipelotrichaceae, Streptococcaceae, Burkholderiaceae and Desulfovibrionaceae were enriched, while Lactobacillaceae and Helicobacteraceae were less abundant. In addition, Desulfovibrionaceae and Streptococcaceae were significantly more abundant in the Pre-Post-Mox mice than in the Pre-Mox and Post-Mox mice. Helicobacteraceae and Rikenellaceae were significantly less abundant in the Pre-Post-Mox mice than in the Pre-Mox or Post-Mox mice ($P < 0.05$, **Figure 7A**). At the genus level, the population of Enterococcus was significantly increased in the Pre-Mox group compared with their levels in the MC mice. Post-Mox mice had relatively higher

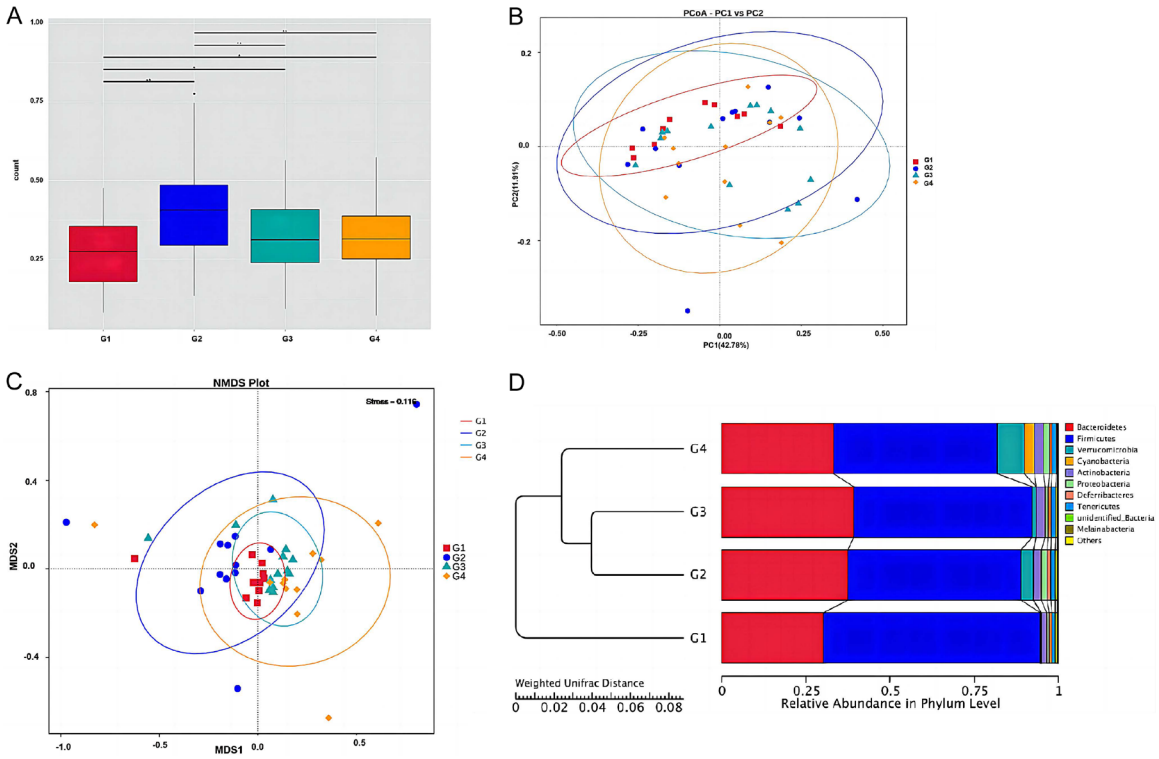

Figure 5. β-diversity analysis and the relative abundance of the top 10 gut microbes in G1, G2, G3 and G4 groups. A. Microbial count, *P < 0.05; **P < 0.01. Overall effects were identified by a Kruskal-Wallis test, and the different effects among treatments were determined by pairwise Wilcoxon rank-sum tests. B. Weighted unifrac PCoA. C. Non-metric Multidimensional scaling (NMDS) plot based on weighted uniFrac distances calculated using OTU compositions. Stress values < 0.2 were considered good after dimensionality reduction. D. The relative abundance of the top 10 microbial taxa was determined at the phylum level. PCoA: principal coordinate analysis; NMDS, non-metric multidimensional scaling. G1: MC group; G2: Pre-Mox group; G3: Post-Mox group; G4: Pre-Post-Mox group.

levels of Erysipelatoclostridium, Enterorhabdus, Lactococcus, Enterococcus, and Parasutterella, as well as lower levels of Bifidobacterium, Helicobacter, Anaerotruncus, Gordonibacter, and Acetatifactor. Akkermansia, Lactococcus, unidentified Erysipelotrichaceae, Parasutterella, and Flavonifractor were more abundant, whereas Lactobacillus, Helicobacter, Rikenella, and Faecalitalea was reduced in Pre-Post-Mox group ($P < 0.05$). Compared with those in the Pre-Mox group, the relative abundance of Lactococcus in the Post-Mox mice and Robinsoniella and Lactococcus in the Pre-Post-Mox mice were increased ($P < 0.05$). In contrast, the abundance of Faecalitalea and Flavonifractor was significantly increased in the Pre-Post-Mox mice compared to that in Post-Mox group ($P < 0.05$, **Figure 7B**).

When we analyzed the differences in species, only the abundance of Enterococcus durans in the Pre-Mox and Post-Mox groups, as well as the abundance of Akkermansia muciniphila, Cocleatum innocuum, and Ruminococcus gauvreauii in the Pre-Post-Mox group were significantly increased compared with their levels in the control group. Furthermore, we found that Lactobacillus gasseri, Lactobacillus reuteri, Helicobacter hepaticus, Lachnospiraceae bacterium, Alistipes finegoldii, Papyrosolvens, and Ruminococcus gauvreauii were enriched in the MC mice ($P < 0.05$). When comparing the mice among different moxibustion treatment groups, the relative abundance of Lachnospiraceae bacterium and Clostridium were significantly lower in the Post-Mox and Pre-Post-Mox groups than in the Pre-Mox group, whereas the levels of Robinsoniella peoriensis and Ruminococcus gauvreauii were relatively higher in the Pre-Post-Mox group. The levels of Alistipes finegoldii, Clostridium leptum, Clostridium papyrosolvens and Dorea were significantly reduced while the level of Ruminococcus_gauvreauii was increased in the Pre-Post-Mox group com-

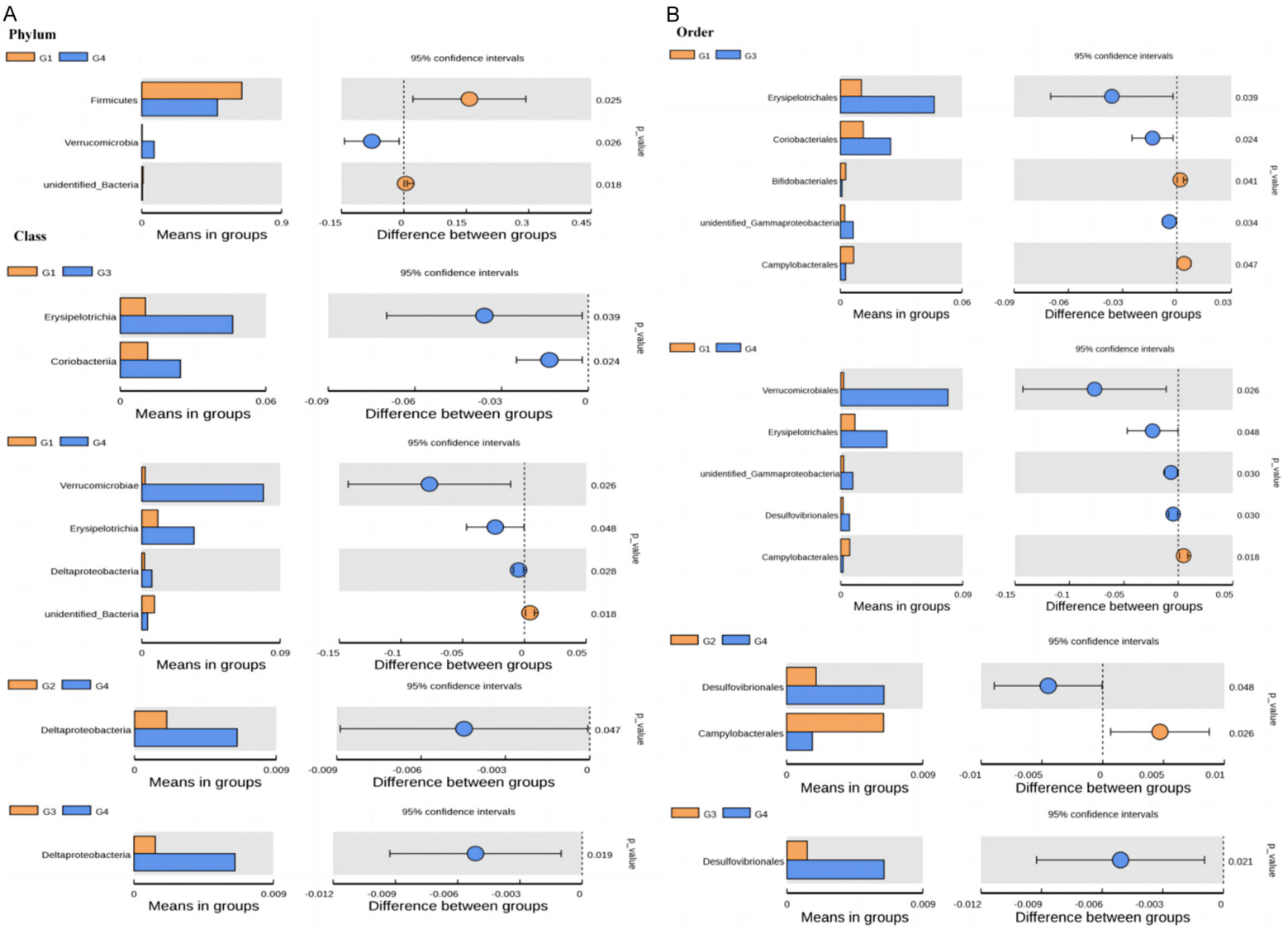

Figure 6. Proportion difference of gut microbiota composition by Student's t test bar plot among the G1, G2, G3 and G4 groups at the phylum, class, and order levels. Bars on the left represent the proportion of each category. Categories difference with a *p* value of <.05 were considered to be significant, and only significant pairwise differences were visualized. A. T-test bar plot on phylum and class level. Significantly enriched species in G1 vs. G2 on phylum level, and G1 vs. G3, G1 vs. G4, G2 vs. G4, G3 vs. G4. on class level. B. T-test bar plot on order level. Significantly enriched species in G1 vs. G3, G1 vs. G4, G2 vs. G4, G3 vs. G4. G1: MC group; G2: Pre-Mox group; G3: Post-Mox group; G4: Pre-Post-Mox group.

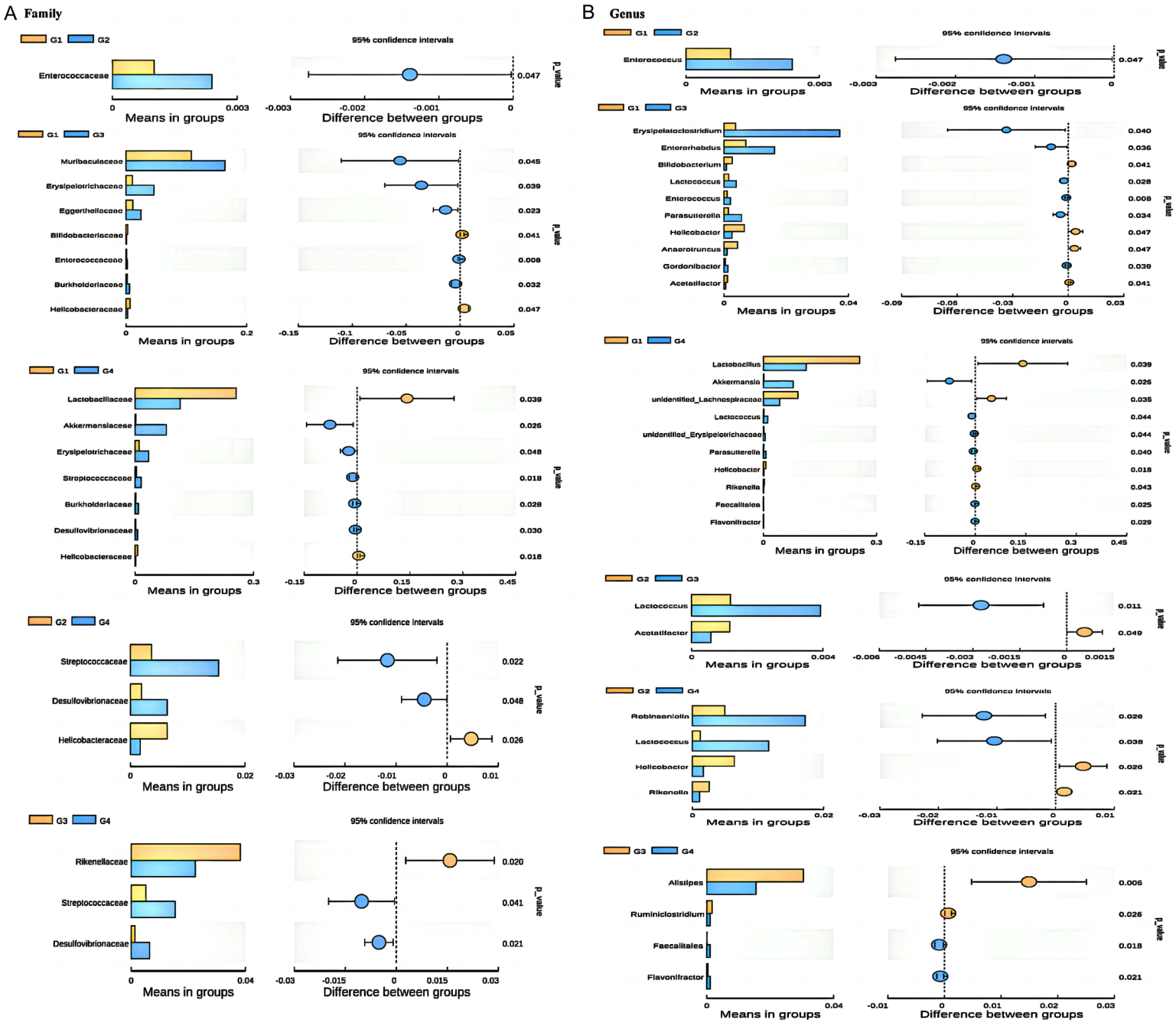
A Family
G1 G2
Enterococcaceae
95% confidence intervals
0.047
Means in groups
Difference between groups
p_value
G1 G3
Muribaculaceae
Erysipelotrichaceae
Eggerthellaceae
Bifidobacteriaceae
Enterococcaceae
Burkholderiaceae
Helicobacteraceae
0.045
0.039
0.023
0.041
0.008
0.032
0.047
G1 G4
Lactobacillaceae
Akkermansiaceae
Erysipelotrichaceae
Streptococcaceae
Burkholderiaceae
Desulfovibrionaceae
Helicobacteraceae
0.039
0.026
0.048
0.018
0.028
0.030
0.018
G2 G4
Streptococcaceae
Desulfovibrionaceae
Helicobacteraceae
0.022
0.048
0.026
G3 G4
Rikenellaceae
Streptococcaceae
Desulfovibrionaceae
0.020
0.041
0.021
B Genus
G1 G2
Enterococcus
0.047
G1 G3
Erysipelatoclostridium
Enterorhabdus
Bifidobacterium
Lactococcus
Enterococcus
Parasutterella
Helicobacter
Anaerotruncus
Gordonibacter
Acetatifactor
0.040
0.036
0.041
0.028
0.008
0.034
0.047
0.047
0.039
0.041
G1 G4
Lactobacillus
Akkermansia
unidentified_Lachnospiraceae
Lactococcus
unidentified_Erysipelotrichaceae
Parasutterella
Helicobacter
Rikenella
Faecalitalea
Flavonifractor
0.039
0.026
0.035
0.044
0.044
0.040
0.018
0.043
0.025
0.029
G2 G3
Lactococcus
Acetatifactor
0.011
0.049
G2 G4
Robinsoniella
Lactococcus
Helicobacter
Rikenella
0.026
0.038
0.026
0.021
G3 G4
Alistipes
Ruminiclostridium
Faecalitalea
Flavonifractor
0.006
0.026
0.018
0.021

Figure 7. Proportion difference of gut microbiota composition by Student's t test bar plot among the G1, G2, G3 and G4 groups at the family and genus levels. Bars on the left represent the proportion of each category in the data. Categories difference with a *p* value of < 0.05 were considered to be significant, and only significant pairwise differences were visualized. A. T-test bar plot on family level. Significantly enriched species from top to bottom in G1 vs. G2, G1 vs. G3, G1 vs. G4, G2 vs. G4, and G3 vs. G4. B. T-test bar plot on genus level. Significantly enriched species in G1 vs. G2, G1 vs. G3, G1 vs. G4, G2 vs. G3, G2 vs. G4, and G3 vs. G4. G1: MC group; G2: Pre-Mox group; G3: Post-Mox group; G4: Pre-Post-Mox group.

pared with those in the Post-Mox group ($P < 0.05$, **Figure 8**).

Discussion

In this study, we showed that moxibustion stimulation could inhibit the liver metastasis of colon cancer cells, and the approach of Pre-Post-Mox treatment had the best effect. In addition, moxibustion at the BL18 and ST36 acupoints altered the microbiota diversity and composition, i.e., Akkermansia muciniphila and Lactobacillus reuteri were significantly enriched.

In China, traditional Chinese medicine plays an important role in cancer prevention and treatment [15]. Recent studies have highlighted the importance of moxibustion as a supplementary therapy during the entire course of treatment, not just for the terminal stage of cancer [16, 17]. Previously, we reported that acupuncture or moxibustion were applied to colon cancer patients mostly via Zusanli, Shenque, Guanyuan, and Qihai points, while Zusanli is most frequently used to relieve the pain from various types of cancer [18]. Zusanli has been reported to enhance the immune response and help maintain the homeostasis of human body [19, 20]. In addition, Ganshu is a well-known acupuncture point for the treatment of liver cancer, viral hepatitis, and depression [18]. Moxibustion at acupuncture point BL18 can inhibit precancerous lesion growth, promote hepatocyte generation, and reduce the expression of apoptosis inhibitors, thereby enhancing the apoptosis of liver cancer cells and inhibiting the growth of liver cancer [21-23].

In this study, we evaluated the efficacy of moxibustion in inhibiting CRC liver metastasis. We found that moxibustion decreased the CRC liver metastasis when administered at 2 weeks before CRC cell injection, or after CRC cell injection for 3 weeks, or when administered at 2 weeks before plus 3 weeks after CRC cell injection (for a total of 5-week treatment). Notably, our results indicated mice in the Pre-Post-Mox group receiving 5-week moxibustion treatment had the highest survival rate. In this study, we used the liver metastasis model via splenic injection of colon cancer cells which can mimic the clinical process in the development and occurrence of CRC liver metastasis, as well as avoid death from late intestinal obstruction from direct inoculation on colon, thereby reducing the death possibility. In addition, this model is easy to perform with a high success rate [24].

The U.S. Food and Drug Administration (FDA) has approved hyperthermia as a clinical treatment for tumors in 1985. Hyperthermia is often used as an adjunct to surgery, chemotherapy, and radiotherapy. As a means of hyperthermia, moxibustion has the function of warming and tonifying. Since normal tissues and the tumor microenvironment have different thermal sensitivity, hyperthermia can be used to kill cancer cells, while producing minimal damage to normal tissues.

Several studies have reported that microbiota alteration affects the development of CRC [25]. A recent research has demonstrated that Bacteroides fragilis and Erysipelotrichaceae in the ileum are involved in the protective immune responses against colon cancer [26]. Furthermore, it has been well known that an unbalanced microbial environment may trigger or promote colorectal tumorigenesis [27], and daily consumption of probiotics has been shown to restore the balance of the microbial community and inhibit the colonization of carcinogenic pathogens in the intestinal tract [28].

Consistently, we observed the direct role of gut microbiota in mediating the suppressive effect of moxibustion. Our results showed that the gut microbiota diversity was significantly altered after moxibustion intervention. It is plausible that the enrichment of probiotic species (i.e., Akkermansia muciniphila, Lactobacillus reuteri) by moxibustion contributes to decreased CRC liver metastasis. In line with this notion, Akkermansia muciniphila, an intestinal symbi-

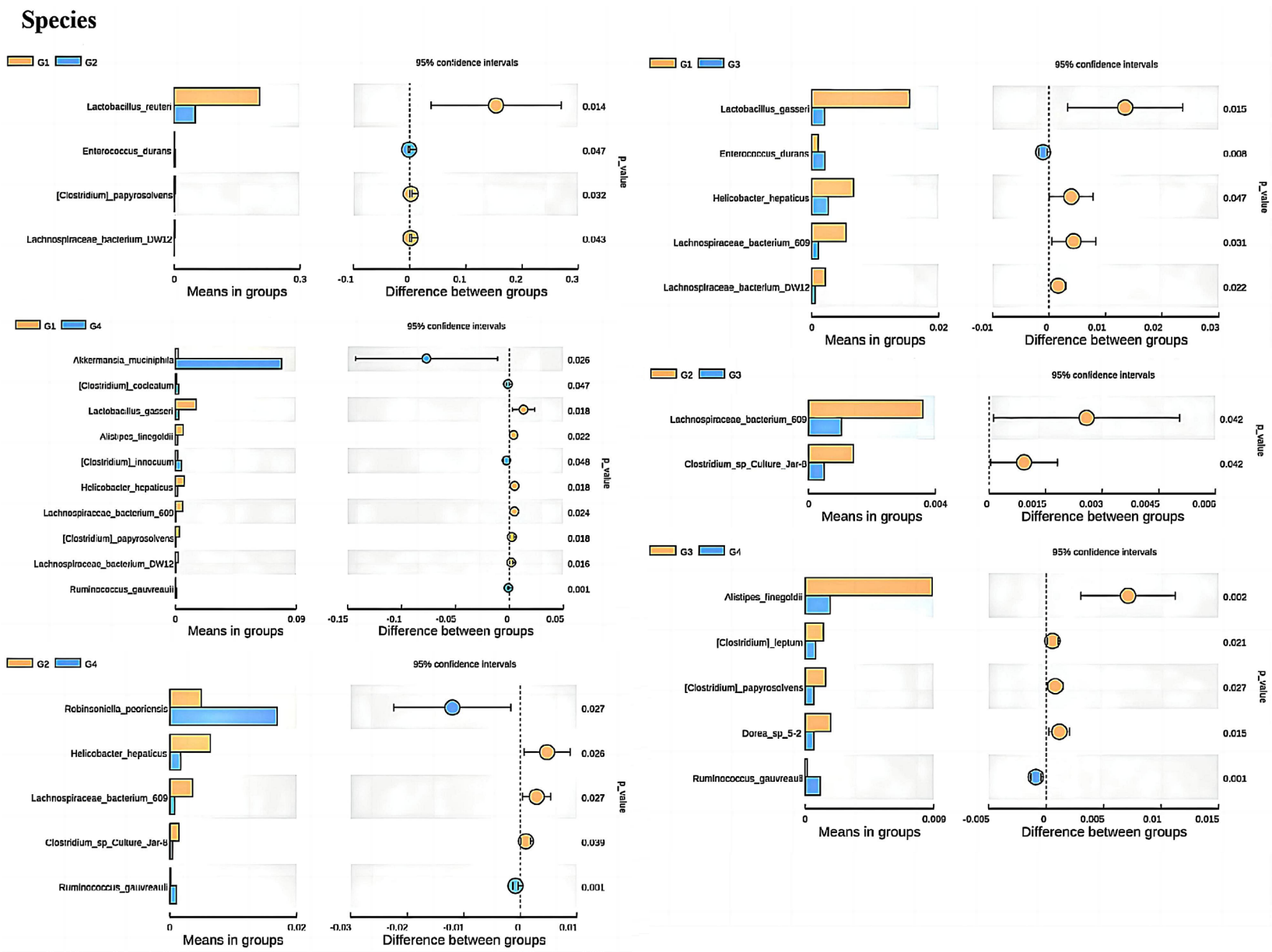
Species
G1 G2
95% confidence intervals
Lactobacillus_reuteri
Enterococcus_durans
[Clostridium]_papyrosolvens
Lachnospiraceae_bacterium_DW12
0.014
0.047
0.032
0.043
p_value
Means in groups
Difference between groups
G1 G3
95% confidence intervals
Lactobacillus_gasseri
Enterococcus_durans
Helicobacter_hepaticus
Lachnospiraceae_bacterium_609
Lachnospiraceae_bacterium_DW12
0.015
0.008
0.047
0.031
0.022
p_value
Means in groups
Difference between groups
G1 G4
95% confidence intervals
Akkermansia_muciniphila
[Clostridium]_cocleatum
Lactobacillus_gasseri
Alistipes_finegoldii
[Clostridium]_innocuum
Helicobacter_hepaticus
Lachnospiraceae_bacterium_609
[Clostridium]_papyrosolvens
Lachnospiraceae_bacterium_DW12
Ruminococcus_gauvreauii
0.026
0.047
0.018
0.022
0.048
0.018
0.024
0.018
0.016
0.001
p_value
Means in groups
Difference between groups
G2 G3
95% confidence intervals
Lachnospiraceae_bacterium_609
Clostridium_sp_Culture_Jar-8
0.042
0.042
p_value
Means in groups
Difference between groups
G2 G4
95% confidence intervals
Robinsoniella_peoriensis
Helicobacter_hepaticus
Lachnospiraceae_bacterium_609
Clostridium_sp_Culture_Jar-8
Ruminococcus_gauvreauii
0.027
0.026
0.027
0.039
0.001
p_value
Means in groups
Difference between groups
G3 G4
95% confidence intervals
Alistipes_finegoldii
[Clostridium]_leptum
[Clostridium]_papyrosolvens
Dorea_sp_5-2
Ruminococcus_gauvreauii
0.002
0.021
0.027
0.015
0.001
p_value
Means in groups
Difference between groups

Figure 8. Proportion difference of gut microbiota composition by Student's t test bar plot among the G1, G2, G3 and G4 groups at the species level. Bars on the left represent the proportion of each category. Categories difference with a p value of < 0.05 were considered to be significant, and only significant pairwise differences were visualized. Significantly enriched species in G1 vs. G2, G1 vs. G3, G1 vs. G4, G2 vs. G3, G2 vs. G4, and G3 vs. G4. G1: MC group; G2: Pre-Mox group; G3: Post-Mox group; G4: Pre-Post-Mox group.

ont colonizing in the mucosal layer, is considered as a promising probiotic candidate which can improve the efficacy of cancer immunotherapy [29] as it can simply remove antibiotics from patients with cancer and increase the effectiveness of PD-1 immunotherapy from 25 to 40%. This obviously allows more cancer patients to benefit from immunotherapy [25]. Probiotic bacteria are defined as "live microorganisms when consumed in sufficient amounts exert health benefits to the host", and Lactobacillus belongs to the lactic acid bacteria (LAB). Many studies have suggested a preventive role of LAB probiotics in the onset of CRC both in vitro and in vivo [25, 30]. In addition, emerging evidence has indicated that the probiotics exert their beneficial effects on CRC prevention though improving the host's immune response, inducing apoptosis, and inhibiting oncogenic tyrosine kinase signaling pathways. For example, several studies have shown that Lactobacillus is able to modulate the expression of genes involved in cell proliferation, apoptosis, and metastasis [31].

Nevertheless, several questions remain to be investigated. First, we identified several microbes as potential biomarkers for CRC liver metastasis; however, the mechanisms underlying the effects of these microbes, especially Akkermansia muciniphila, one of the most abundant bacteria, remain to be elucidated. Our current study was only a preliminary exploration of the relationship between moxibustion and microbiota; hence, we also did not intervene with the gut microbial diversity, either by replenishing or destructing Akkermansia muciniphila. Further studies are needed to investigate how moxibustion alters gut microbiota diversity and to investigate the functions of Akkermansia muciniphila in CRC liver metastasis. Second, although the 5-week Pre-Post-Mox treatment showed the best inhibitory effect on CRC liver metastasis, the association between the gut microbiota and Pre-Post-Mox intervention remains to be determined which warrants further investigation. Lastly, our conclusion needs to be verified in randomized controlled human clinical studies.

Conclusion

In conclusion, this study was the first to demonstrate that moxibustion could exert an inhibitory effect on CRC liver metastasis. The potential mechanism might rely on the alteration of microbiota diversity and composition, such as the enrichment of Akkermansia muciniphila and Lactobacillus to clear colon cancer cells. This finding indicates that moxibustion might target the microbiome structure among its multiple targets when used in the treatment of patients with CRC liver metastasis.

Acknowledgements

This project was financially supported by the National Natural Science Fund (grant numbers 82274630 and 82174489), the Youth Talent Project of Jiangsu Province Traditional Chinese Medicine Science and Technology (grant number QN202101), the Peak Talent Project of Jiangsu Province Hospital of Chinese Medicine (grant numbers y2018rc05 and y2018rc25). The authors would like to thank the management of Dongnan University for providing the required infrastructure to complete the research work.

Disclosure of conflict of interest

None.

Address correspondence to: Li-Xia Pei and Jian-Hua Sun, Department of Acupuncture Rehabilitation, Affiliated Hospital of Nanjing University of Chinese Medicine, No. 155, Hanzhong Road, Qinhuai District, Nanjing, Jiangsu, P. R. China. Tel: +86 25-8661-7141; Fax: +86 25-8661-0925; E-mail: fsyy00663@njucm.edu.cn (LXP); E-mail: fsyy00657@njucm.edu.cn (JHS)

References

[1] Choti MA, Thomas M, Wong SL, Eaddy M, Pawlik TM, Hirose K,Weiss MJ, Kish J, Mark R and Green MR. Surgical resection preferences and perceptions among medical oncologists treating liver metastases from colorectal cancer. Ann Surg Oncol 2016; 23: 375-381.

[2] D'Angelo E, Natarajan D, Sensi F, Ajayi O, Fassan M, Mammano E, Pilati P, Pavan P, Bresolin S, Preziosi M, Miquel R, Zen Y, Chokshi S, Menon K, Heaton N, Spolverato G, Piccoli M, Williams R, Urbani L and Agostini M. Patient-derived scaffolds of colorectal cancer metastases as an organotypic 3D model of the liver metastatic microenvironment. Cancers (Basel) 2020; 12: 364.

[3] Cervantes A, Adam R, Roselló S, Arnold D, Normanno N, Taïeb J, Seligmann J, Baere TD, Osterlund P, Yoshino T and Martinelli E; ESMO Guidelines Committee. Metastatic colorectal cancer: ESMO clinical practice guidelines for diagnosis, treatment and follow-up. Ann Oncol 2023; 34: 10-32.

[4] Aloia TA, Vauthey JN, Loyer EM, Ribero D, Pawlik TM, Wei SH, Curley SA, Zorzi D and Abdalla EK. Solitary colorectal liver metastasis: resection determines outcome. Arch Surg 2006; 141: 460-6; discussion 466-7.

[5] Phipps O, Al-Hassi HO, Quraishi MN, Kumar A and Brookes MJ. Influence of Iron on the gut microbiota in colorectal cancer. Nutrients 2020; 12: 2512.

[6] Zhao R, Coker OO, Wu J, Zhou Y, Zhao L, Nakatsu G, Bian X, Wei H, Chan AWH, Sung JJY, Chan FKL, El-Omar E and Yu J. Aspirin reduces colorectal tumor development in mice and gut microbes reduce its bioavailability and chemopreventive effects. Gastroenterology 2020; 159: 969-983, e4.

[7] Li X, Guo G, Shen F, Kong L, Liang F and Sun G. Moxibustion activates macrophage autophagy and protects experimental mice against bacterial infection. Evid Based Complement Alternat Med 2014; 2014: 450623.

[8] Qin PL and Cheng ZD. The thinking of discussion of acupuncture and moxibustion for regulating intestinal flora based on brain-gut axis theory. Shi Zhen Guo Yi Guo Yao 2015; 26: 2712-2714.

[9] Wei D, Xie L, Zhuang Z, Zhao N, Huang B, Tang Y, Yu S, Zhou Q and Wu Q. Gut microbiota: a new strategy to study the mechanism of electroacupuncture and moxibustion in treating ulcerative colitis. Evid Based Complement Alternat Med 2019; 2019: 9730176.

[10] Qi Q, Liu YN, Jin XM, Zhang LS, Wang C, Bao CH, Liu HR, Wu HG and Wang XM. Moxibustion treatment modulates the gut microbiota and immune function in a dextran sulphate sodium-induced colitis rat model. World J Gastroenterol 2018; 24: 3130-3144.

[11] Kitamura T, Fujishita T, Loetscher P, Revesz L, Hashida H, Kizaka-Kondoh S, Aoki M and Taketo MM. Inactivation of chemokine (C-C motif) receptor 1 (CCR1) suppresses colon cancer liver metastasis by blocking accumulation of immature myeloid cells in a mouse model. Proc Natl Acad Sci U S A 2010; 107: 13063-13068.

[12] Shimma S, Sugiura Y, Hayasaka T, Hoshikawa Y, Noda T and Setou M. MALDI-based imaging mass spectrometry revealed abnormal distribution of phospholipids in co*lon can*cer liver metastasis. J Chromatogr B Analyt Technol Biomed Life Sci 2007; 855: 98-103.

[13] Li ZR. Experimental Acupuncture 2ed. Chinese Press of Traditional Chinese Medicine 2007. pp. 255-257.

[14] Parada AE, Needham DM and Fuhrman JA. Every base matters: assessing small subunit rRNA primers for marine microbiomes with mock communities, time series and global field samples. Environmental Microbiology 2016; 18: 1403-1414.

[15] Lin H, Liu J and Zhang Y. Developments in cancer prevention and treatment using traditional Chinese medicine. Front Med 2011; 5: 127-133.

[16] Li Z, Zheng Z, Wang L, Xiao W, Zeng J, Hao J, Chen R and Xie D. Efficacy evaluation of heat-sensitive moxibustion for chemotherapy symptoms of large intestine cancer. Zhongguo Zhen Jiu 2015; 35: 1010-1013.

[17] Zheng Y, He NY, Zhang YP and Wang XL. Observations on the efficacy of thunder-fire wonder moxibustion plus Chinese and western medications in treating myelosuppression after chemotherapy for colorectal cancer. Shanghai Journal of Acupuncture and Moxibustion 2019; 38: 1233-1238

[18] Chen AW, Li YJ, Ma W and Shen WD. Study on data mining of acupoints selection in acupuncture treatment of cancer pain based on traditional Chinese medicine inheritance support system. Shanghai Journal of Traditional Chinese Medicine 2017; 51: 16-20.

[19] Fu H, Chen B, Hong S and Guo Y. Acupuncture therapy for the treatment of myelosuppression after chemotherapy: a literature review over the past 10 years. J Acupunct Meridian Stud 2015; 8: 122-126.

[20] Wang Z, Chen T, Long M, Chen L, Wang L, Yin N and Chen Z. Electro-acupuncture at acupoint ST36 ameliorates inflammation and regulates Th1/Th2 balance in delayed-type hypersensitivity. Inflammation 2017; 40: 422-434.

[21] Wang P, Zhu J, Xie XL, Sui MH, Zhang QJ, Jia WR, Xin SY, Liu Y and Hou ZW. Effects on the tumor specific growth factor and tumor necrosis factor alpha in rats' precancerous lesion of primary hepatocellular carcinoma by direct moxibustion at Ganshu (BL 18) acupoint. Chin J Integr Med 2016; 22: 532-536.

[22] Cheng YZ. Effect of direct moxibustion at "Ganshu" point on TSGF and Livin in HCC rats

[D]. Beijing University of traditional Chinese Medicine 2017.
[23] Yan YN, Wang N, Wang ZY, Tian Y, Cheng YZ, Ma HF, Hou ZW, Ma JJ and Guan HY. Effects of direct moxibustion of "Ganshu" (BL 18) on the contents of T cells in peripheral blood in rats with precancerous lesion of primary hepatocellular carcinoma. Zhen Ci Yan Jiu 2016; 41: 321-326.
[24] Zhou JY, Chen M, Wu CE, Zhuang YW, Chen YG and Liu SL. The modified Si-Jun-Zi decoction attenuates colon cancer liver metastasis by increasing macrophage cells. BMC Complement Altern Med 2019; 19: 86.
[25] Routy B, Le Chatelier E, Derosa L, Duong C, Alou MT, Daillere R, Fluckiger A, Messaoudene M, Rauber C, Roberti MP, Fidelle M, Flament C, Poirier-Colame V, Opolon P, Klein C, Iribarren K, Mondragón L, Jacquelot N, Qu B, Ferrere G, Clémenson C, Mezquita L, Masip JR, Naltet C, Brosseau S, Kaderbhai C, Richard C, Rizvi H, Levenez F, Galleron N, Quinquis B, Pons N, Ryffel B, Minard-Colin V, Gonin P, Soria JC, Deutsch E, Loriot Y, Ghiringhelli F, Zalcman G, Goldwasser F, Escudier B, Hellmann MD, Eggermont A, Raoult D, Albiges L, Kroemer G and Zitvogel L. Gut microbiome influences efficacy of PD-1-based immunotherapy against epithelial tumors. Science 2018; 359: 91-97.
[26] Roberti MP, Yonekura S, Duong C, Picard M, Ferrere G, Tidjani AM, Rauber C, Lebba V, Lehmann CHK, Amon L, Dudziak D, Derosa L, Routy B, Flament C, Richard C, Daillère R, Fluckiger A, Seuningen IV, Chamaillard M, Vincent A, Kourula S, Opolon P, Ly P, Pizzato E, Becharef S, Paillet J, Klein C, Marliot F, Pietrantonio F, Benoist S, Scoazec JY, Dartigues P, Hollebecque A, Malka D, Pagès F, Galon J, Boneca IG, Lepage P, Ryffel B, Raoult D, Eggermont A, Berghe TV, Ghiringhelli F, Vandenabeele P, Kroemer G and Zitvogel L. Chemotherapy-induced ileal crypt apoptosis and the ileal microbiome shape immunosurveillance and prognosis of proximal colon cancer. Nat Med 2020; 26: 919-931.
[27] Wong SH and Yu J. Gut microbiota in colorectal cancer: mechanisms of action and clinical applications. Nat Rev Gastroenterol Hepatol 2019; 16: 690-704.
[28] Rafter J, Bennett M, Caderni G, Clune Y, Hughes R, Karlsson PC, Klinder A, O'Riordan M, O'Sullivan GC, Pool-Zobel B, Rechkemmer G, Roller M, Rowland L, Salvadori M, Thijs H, Loo JV, Watzl B and Collins JK. Dietary synbiotics reduce cancer risk factors in polypectomized and colon cancer patients. Am J Clin Nutr 2007; 85: 488-496.
[29] Dingemanse C, Belzer C, van Hijum SA, Gunthel M, Salvatori D, den Dunnen JT, Kuijper EJ, Devilee P, de Vos WM, van Ommen GB and Robanus-Maandag EC. Akkermansia muciniphila and helicobacter typhlonius modulate intestinal tumor development in mice. Carcinogenesis 2015; 36: 1388-1396.
[30] Tiptiri-Kourpeti A, Spyridopoulou K, Santarmaki V, Aindelis G, Tompoulidou E, Lamprianidou EE, Saxami G, Ypsilantis P, Lampri ES, Simopoulos C, Kotsianidis L, Galanis A, Kourkoutas Y, Dimitrellou D and Chlichlia K. Lactobacillus casei exerts anti-proliferative effects accompanied by apoptotic cell death and up-regulation of TRAIL in colon carcinoma cells. PLoS One 2016; 11: e147960.
[31] Nowak A, Paliwoda A and Blasiak J. Anti-proliferative, pro-apoptotic and anti-oxidative activity of lactobacillus and bifidobacterium strains: a review of mechanisms and therapeutic perspectives. Crit Rev Food Sci Nutr 2019; 59: 3456-3467.